Near infrared spectroscopy of benzoic acid adsorbed on montmorillonite

Longfei Lu, [1,2] Jingong Cai [2] and Ray L. Frost [1*]

[1] Inorganic Materials Research Program, School of Physical and Chemical Sciences, Queensland University of Technology, GPO Box 2434, Brisbane Queensland 4001, Australia.

[2] State Key Laboratory of Marine Geology, Tongji University, Shanghai 200092, China

Abstract

The adsorption of benzoic acid on both sodium and calcium montmorillonites has been studied by near infrared spectroscopy complimented with infrared spectroscopy. Upon adsorption of benzoic acid additional near infrared bands are observed at 8665 cm^{-1} and assigned to an interaction of benzoic acid with the water of hydration. Upon adsorption of the benzoic acid on Na-Mt, the NIR bands are now observed at 5877, 5951, 6028 and 6128 cm^{-1} and are assigned to the overtone and combination bands of the CH fundamentals. Additional bands at 4074, 4205, 4654 and 4678 cm^{-1} are attributed to CH combination bands resulting from the adsorption of the benzoic acid. Benzoic acid is used as a model molecule for adsorption studies. The application of near infrared spectroscopy to the study of adsorption has the potential for the removal of acids from polluted aqueous systems.

Keywords: montmorillonites, benzoic acid, near infrared spectroscopy, adsorption, structured water

[*] Corresponding author: Ray Frost
Email address: r.frost@qut.edu.au
Address: 2 George Street, Brisbane Q 4001, Australia

Introduction

Smectites are widely used in a range of applications because of their high cation exchange capacity, swelling capacity, high surface area and resulting strong adsorption/absorption capacities. One highly utilized application is the use of clays as adsorbents. In expanding clays, the most common dioctahedral smectite is montmorillonite, which has two silica-oxygen tetrahedral sheets sandwiching an aluminium or magnesium octahedral sheet, where an aluminium or magnesium ion is octahedrally coordinated to six oxygens or hydroxyls. Because of substitution of silicon by aluminium in the tetrahedral layers or similar substitution of aluminium by magnesium, montmorillonite layers are negatively charged [1-4]. Thus, cations like sodium, potassium and calcium are attracted to the mineral interlayer space to neutralize the negative layer charges. Because of the hydration of inorganic cations on the exchange sites, the clay mineral surface is hydrophilic in nature [5, 6]. This makes natural clays suitable as effective sorbents for organic compounds.

At present, there are many applications of montmorillonites as sorbents in pollution prevention and environmental remediation such as treatment of spills, waste water and hazardous waste landfills [7-16]. Some studies have showed that replacing the inorganic exchange cations of clay minerals with organic cations can result in greatly enhanced capacity of these materials to remove organic contaminants from soils and industrial effluents [17, 18]. The use of NIR spectroscopy for the determination of minerals was first elucidated by Hunt et al. [19-25]. NIR spectroscopy has been applied to clay minerals [26-30]. NIR spectroscopy has proven particularly useful for soil analysis [31, 32]. To date there have been few reports of the use of NIR spectroscopy to determine the adsorption of organic molecules on clays and organoclays [33].

In this work we extend these adsorption studies to the determination of adsorbed benzoic acid on montmorillonite. Montmorillonite clay was chosen as the model adsorbent on basis of the following reasons: 1) it is used widely in agriculture, dyes/pigments, engineering polymers and pharmaceuticals and as fungicide for leather, production of parathion and organic synthesis [34] and 2) US Environmental

Protection Agency (USEPA) claimed the organic acids as one of the main organic contaminations [35]. Our present study demonstrates that NIR is a powerful technique to determine the adsorption of these organic pollutants on clay and the resulting clay materials. It is of high importance to understand well the adsorption mechanism of clay materials to organic pollutants and for the application of clay-based materials in pollution prevention and environmental remediation.

Experimental

Materials

The montmorillonites used in this study were supplied by The Clay Mineral Society and were standard minerals labeled as SWy-2 (Na-rich montmorillonite) Crook County, Wyoming, USA and STx-1 (Ca-Montmorillonite, white) Gonzales County, Texas, USA.

Method of adsorption

5g benzoic acid were dissolved and made up to 300ml with toluene. 10g Ca/Na montmorillonite were weighted into a 500ml an ampoule. 250ml of the acid solution were pipetted into the ampoule with a magnetic stir bar. The samples were stirred for 8h in in 35±2 °C. The solids were recovered by centrifugation, washed once with toluol, twice with ethanol, and thereafter once with acetone. After each washing the solids were separated from the liquid by centrifugation. The product was allowed to dry at room temperature.

Near and Mid Infrared Spectroscopy

NIR spectra in reflectance mode use a Nicolet Nexus FT-IR spectrometer with a Nicolet Near-IR Fibreport accessory (Nicolet Nexus, Madison, Wisconsin, USA). A white light source was used, with a quartz beam splitter and TEC NIR InGaAs detector. Spectra were obtained from 12 000 to 4000 cm^{-1} (909 – 2,500 nm) by the co-addition of 64 scans at a resolution of 8 cm^{-1}. A mirror velocity of 1.2659 m/s was

used. The spectra were transformed using the Kubelka-Munk algorithm ($f(R_\infty) = (1-R_\infty)^2/2R_\infty$) for comparison with absorption spectra.

Mid-infrared and NIR spectra were obtained using an FT spectrometer ((Nicolet Nexus, Madison, Wisconsin, USA) with a single bounce diamond ATR cell. Spectra over the 4000 to 500 cm^{-1} (2,500 – 20,000 nm) range were obtained by the co-addition of 64 scans with a resolution of 4 cm^{-1} and a mirror velocity of 0.6329 cm/s.

The spectral manipulations of baseline adjustment, smoothing, and normalization were performed using the Spectracalc software package GRAMS (Galactic Industries Corporation, NH, USA). Band component analysis was carried out using Peakfit software (Jandel Scientific, Postfach 4107, D-40688 Erkrath, Germany). Lorentz-Gauss cross product functions were used through out and peak fit analysis undertaken until squared correlation coefficients with R^2 greater than >0.995 were obtained.

Results and Discussion

For convenience, the NIR spectra of montmorillonite (Na-Mt), montmorillonite with adsorbed benzoic acid, calcium montmorillonite with and without adsorbed benzoic acid may be divided into sections according to the spectral region where NIR intensity is observed:

(a) The 7900 to 9100 cm^{-1} region (Fig. 1)

(b) The 5800 to 7400 cm^{-1} region (Fig.2)

(c) 4000 to 5500 cm^{-1} region (Fig. 3).

The infrared spectra of the OH and CH stretching regions of the montmorillonite, montmorillonite with adsorbed benzoic acid are illustrated in Figs 4 and 5 respectively.

NIR spectroscopy is often referred to as proton spectroscopy. Bands which occur in the NIR spectrum are the result of overtone and/or combination bands of bands that are observed in the mid-infrared spectra. Thus the bands in the NIR spectra of the montmorillonite clays with adsorbed benzoic acid will result from the overtones of OH or CH bands. In this experiment the benzoic acid is being used as a model molecule to test the NIR measurement of the adsorption on montmorillonite.

NIR bands in the high wavenumber region between 7900 and 9100 cm^{-1} are shown in Figure 1. For Na-Mt a band is observed at 8667 cm^{-1} and for Ca-Mt two bands are observed at 8530 and 8666 cm^{-1}. One possibility is that these bands are due to electronic transitions, however, this seems unlikely as the clay does not contain any transition metal cations. The assignment of the bands is therefore given to OH combination bands. The band might be due to the combination of $2\nu_1 + 2\delta OH$. This would be approximately 2x3500 + 2x800 = 8600 cm^{-1}. Another alternative is that the bands are due to OH stretching bands combined with water vibrations. One may conclude that the second band at 8530 cm^{-1} is a result of differences in hydration of the calcium in the montmorillonites interlayer. Upon adsorption of the benzoic acid on the Na-Mt an additional band at 8665 cm^{-1} is observed. This additional band is evidence for the interaction of the benzoic acid with the hydroxyl surface or the water of hydration of the cation. Alternatively the benzoic acid has interacted with the hydration sphere of the sodium and this has altered the summation of bands proposed above. In the NIR spectrum for calcium montmorillonite, bands are observed at 6634, 6857, 7070 and 7152 cm^{-1}. These bands are in the region of the first overtone of the OH fundamental and are therefore assigned to bands due to $2\nu_1$, $2\nu_3$, and $\nu_1 + 2\nu_3$.

For the adsorption of benzoic acid on the Ca-Mt additional bands additional bands are observed at 7967, 8292 and there is a shift in the 8530 cm^{-1} band to 8651 cm^{-1}. It is concluded that the benzoic acid has interacted with the water of hydration of the calcium cations in the montmorillonites interlayer.

The NIR spectra in the 5800 to 7400 cm^{-1} are reported in Figure 2. This spectral region is the region of the first overtone of the hydroxyl fundamental and results from $2\nu_1$. It must be remembered that in NIR spectroscopy all combinations of bands are allowed. Thus bands = $2\ \nu_3$ and $\nu_1 + \nu_3$ are allowed. Thus for Na-Mt three bands are observed at 6610, 6835 and 7085 cm^{-1}. Similarly for Ca-Mt three bands are observed at 6634, 6857 and 7070 cm^{-1}. Upon adsorption of the benzoic acid on Na-Mt, the NIR bands of the clay are found at 6822, 6947 and 7083 cm^{-1}. Additional bands are now observed at 5877, 5951, 6028 and 6128 cm^{-1}. These bands are assigned to the overtone and combination bands of the CH fundamentals. These bands are not observed in this spectral region and provide evidence of the adsorption of the benzoic

167 acid on the montmorillonite. A similar set of bands are observed for the ca-Mt with
168 bands at 5879, 5963, 6025 and 6123 cm^{-1}. The bands are in similar positions for both
169 the Na-Mt and Ca-Mt adsorptions.
170
171 The NIR spectra in the 4000 to 5500 cm^{-1} are shown in Figure 3. This spectral
172 region is where combination bands from water and the montmorillonites are found.
173 Three bands are observed for Na-Mt at 4917, 5132 and 5248 cm^{-1} and are attributed to
174 water combination bands. Two bands at 4460 and 4536 cm^{-1} are assigned to OH
175 combination bands from the montmorillonite. For Ca-Mt the water combination bands
176 are found at 4837, 5024, 5165 and 5247 cm^{-1}. The OH combination band is found at
177 4525 cm^{-1}. Upon adsorption of the benzoic acid on Na-Mt additional bands are found
178 at 4074, 4205, 4654 and 4678 cm^{-1}. These bands are attributed to CH combination
179 bands resulting from the adsorption of the benzoic acid. For the Ca-Mt, these
180 additional bands are found at 4073, 4137, 4202, 4368, 4628, 4677 and 4759 cm^{-1}.
181 These additional bands prove the adsorption of benzoic acid on montmorillonites
182 surfaces.
183
184 The infrared spectrum of the Na-Mt and the Ca-Mt with and without the
185 adsorption of benzoic acid is reported in Figure 4. Four bands are observed for Na-Mt
186 at 3221, 3413, 3541 and 3626 cm^{-1}. This latter band is assigned to the inner hydroxyl
187 group of the montmorillonites. The first three bands are attributed to water in the
188 montmorillonite interlayer. A similar set of bands is found for the Ca-Mt. The
189 additional bands are clearly due to the adsorption of benzoic acid. In Figure 5, the
190 spectral region between 1350 and 1800 cm^{-1} is displayed. For Na-Mt, an infrared
191 band is observed at around 1635 cm^{-1} which may be resolved into component bands at
192 1628 and 1649 cm^{-1}. These bands are assigned to the water HOH bending mode. For
193 Ca-Mt, the two bands are found at 1629 and 1660 cm^{-1}. The observation of a higher
194 energy component is indicative of water which is strongly hydrogen bonded such as
195 in the hydration sphere of the Na or Ca ions. The band at 1629 cm^{-1} is assigned to
196 the bending mode of water bonded to water. Upon adsorption of the benzoic acid
197 additional bands are observed as observed in Figure 5. Interestingly the water bending
198 mode is now observed at around 1687 cm^{-1}. This indicates that upon adsorption of
199 the benzoic acid the hydrogen bond between the water in the hydration sphere is
200 stronger. This suggests that the benzoic acid is adsorbed into the interlayer of the

montmorillonites. Such a conclusion fits well with the conclusions of Yariv et al. [36]

In this work we have shown the potential for NIR spectroscopy for the determination of adsorbed acids on montmorillonitic clays. Since many pollutants are acidic, benzoic acid was selected as a molecule to represent these possible pollutants. NIR spectroscopy is a rapid technique which with modern portable hand held spectrometers enables an assessment of pollutants to be quickly made. Other techniques such as X-ray diffraction do not offer such instant results.

Conclusions:

This research has focused on the study of the adsorption of benzoic acid upon sodium and calcium montmorillonites using near infrared spectroscopy. Montmorillonites are noted for their swelling properties and the water of hydration of the cations in the interlayer. Differences in the NIR spectra of sodium and calcium montmorillonites are attributed to the differences in the water in the hydration sphere. This is observed in the hydroxyl combination and first overtones of the OH fundamentals. NIR spectroscopy offers methodology for the easy analysis of acids adsorbed on clays. Other techniques including XRD are not suitable for these adsorption studies.

The adsorption of the benzoic acid is readily observed by comparing the spectra of the montmorillonites with and without adsorbed benzoic acid. The adsorption of benzoic acid results in the observation of additional NIR bands in the 5800 to 6150 cm^{-1} region. NIR bands at 5877, 5951, 6028 and 6128 cm^{-1} are observed. These bands are assigned to overtones of the CH vibrations. Additional NIR bands at 4074, 4205, 4654 and 4678 cm^{-1} are attributed to CH combination bands resulting from the adsorption of the benzoic acid.

Acknowledgements

The financial and infra-structure support of the Queensland University of Technology, Inorganic Materials Research Program of the School of Physical and Chemical Sciences is gratefully acknowledged. The Australian Research Council (ARC) is

235 thanked for funding the scientific facilities. Financial supports from the National
236 Natural Science Foundation of China through Grant Nos: 40672085 and 40872089 are
237 acknowledged.
238
239

References

[1] H.P. He, R.L. Frost, T. Bostrom, P. Yuan, L. Duong, D. Yang, Y.F. Xi, J.T. Kloprogge, Applied Clay Science 31, 262, (2006)

[2] H.P. He, R.L. Frost, Y.F. Xi, J.X. Zhu, Journal of Raman Spectroscopy 35, 316, (2004)

[3] H.P. He, R.L. Frost, F. Deng, J.X. Zhu, X.F. Wen, P. Yuan, Clays and Clay Minerals 52, 350, (2004)

[4] J.T. Kloprogge, S. Komarneni, J.E. Amonette, Clays and Clay Minerals 47, 529, (1999)

[5] Y.F. Xi, R.L. Frost, H.P. He, Journal of Colloid and Interface Science 305, 150, (2007)

[6] N. Pejcinovic, T. Nguyen, R.L. Frost, Colloids and Surfaces A: Physicochemicla and Engineering Aspects 292, 21, (2007)

[7] G. Akcay, K. Yurdakoc, Acta Hydrochimica et Hydrobiologica 28, 300, (2000)

[8] G. Alther, Contaminated Soils 7, 223, (2002)

[9] G.W. Beall, Applied Clay Science 24, 11, (2003)

[10] L. Groisman, C. Rav-Acha, Z. Gerstl, U. Mingelgrin, Journal of Environmental Quality 33, 1930, (2004)

[11] H. Moazed, Report (2000)

[12] V.A. Oyanedel-Craver, J.A. Smith, Journal of Hazardous Materials 137, 1102, (2006)

[13] G. Rytwo, Y. Gonen, Colloids and Polymer Science 284, 817, (2006)

[14] Q. Zhou, H.P. He, P. Yuan, Yanshi Kuangwuxue Zazhi 24, 568, (2005)

[15] G. Abate, L.B.O.D. Santos, S.M. Colombo, J.C. Masini, Applied Clay Science 32, 261, (2006)

[16] G.R. Alther, Water Environment and Technology 13, 31, (2001)

[17] Q. Zhou, R.L. Frost, H.P. He, Y.F. Xi, Journal of Colloid and Interface Science 307, 357, (2007)

[18] Q. Zhou, R.L. Frost, H.P. He, Y.F. Xi, Journal of Colloid and Interface Science 307, 50, (2007)

[19] G.R. Hunt, R.B. Hall, Clays and Clay Minerals 29, 76, (1981)

[20] G.R. Hunt, R.P. Ashley, Economic Geology and the Bulletin of the Society of Economic Geologists 74, 1613, (1979)

[21] J.D. Lindberg, D.G. Snyder, American Mineralogist 57, 485, (1972)
[22] G.R. Hunt, J.W. Salisbury, C.J. Lenhoff, Modern Geology 3, 121, (1972)
[23] G.R. Hunt, J.W. Salisbury, C.J. Lenhoff, Modern Geology 2, 195, (1971)
[24] G.R. Hunt, J.W. Salisbury, Modern Geology 2, 23, (1971)
[25] G.R. Hunt, J.W. Salisbury, Modern Geology 1, 283, (1970)
[26] S. Petit, A. Decarreau, F. Martin, R. Buchet, Physics and Chemistry of Minerals 31, 585, (2004)
[27] J. Madejova, Vibrational Spectroscopy 31, 1, (2003)
[28] J. Madejova, P. Komadel, Clays and Clay Minerals 49, 410, (2001)
[29] R.L. Frost, J.T. Kloprogge, Z. Ding, Spectrochimica Acta, Part A: Molecular and Biomolecular Spectroscopy 58A, 1657, (2002)
[30] J.C. Donini, K.H. Michaelian, Infrared Physics 26, 135, (1986)
[31] K. Islam, B. Singh, A. Mcbratney, Australian Journal of Soil Research 41, 1101, (2003)
[32] L. Kooistra, R. Wehrens, R.S.E.W. Leuven, L.M.C. Buydens, Analytica Chimica Acta 446, 97, (2001)
[33] J. Madejova, H. Palkova, P. Komadel, Vibrational Spectroscopy 40, 80, (2006)
[34] J.H. Montgomery, L.M. Welkom, Groundwater Chemicals Desk Reference, Lewis Publishers, Inc., Chelsea, MI, 1990.
[35] W. Cawley, Treatability Manual. Vol. I. Treatability Data, 1980.
[36] S. Yariv, J.D. Russell, V.C. Farmer, Israel Journal of Chemistry 4, 201-213, (1966)

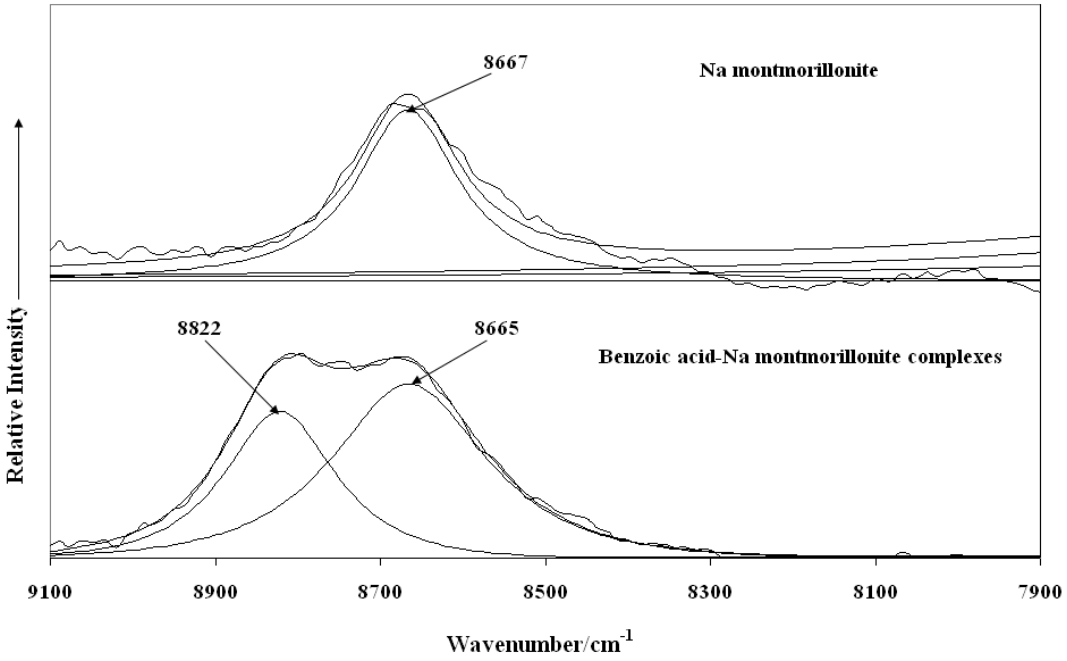

308

309

310 **Figure1a**

311

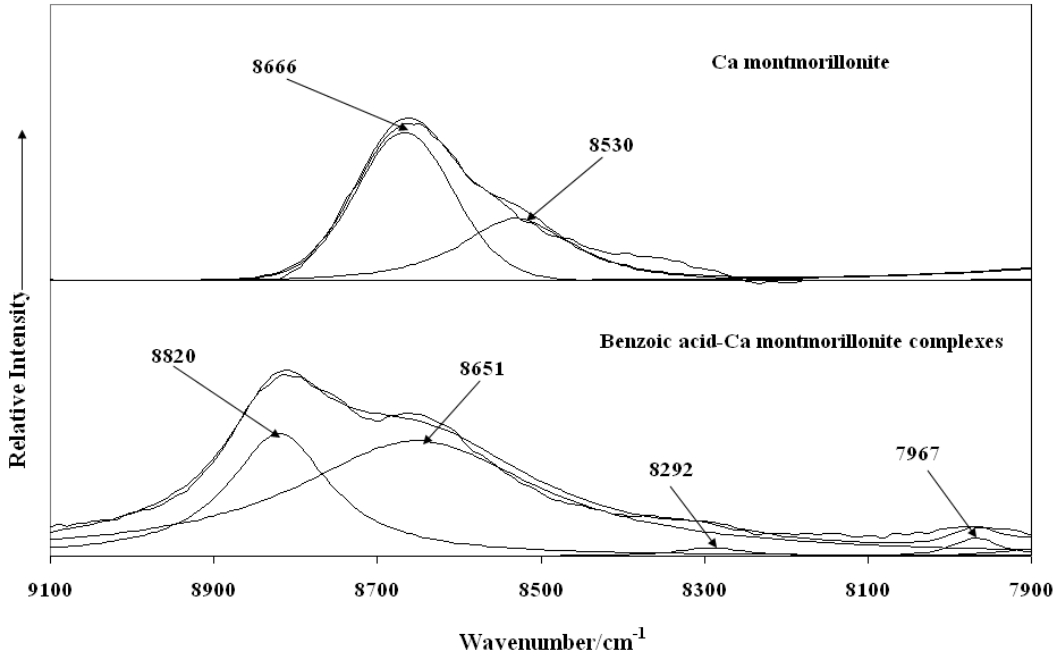

312

313

314 **Figure1b**

315

316

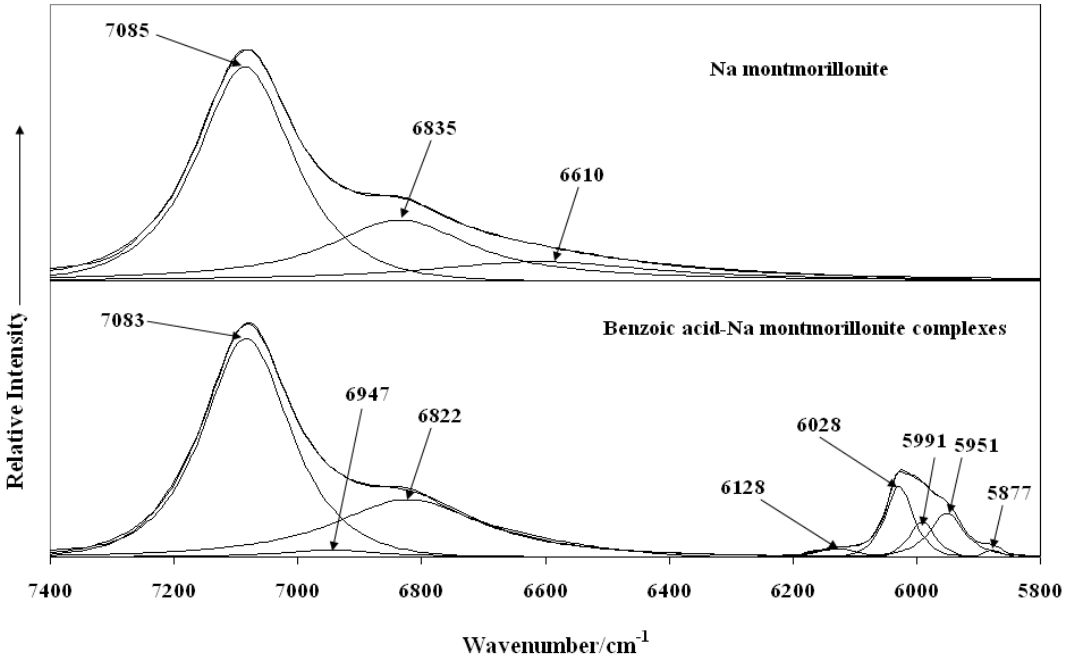

317

318

319 **Figure 2a**

320

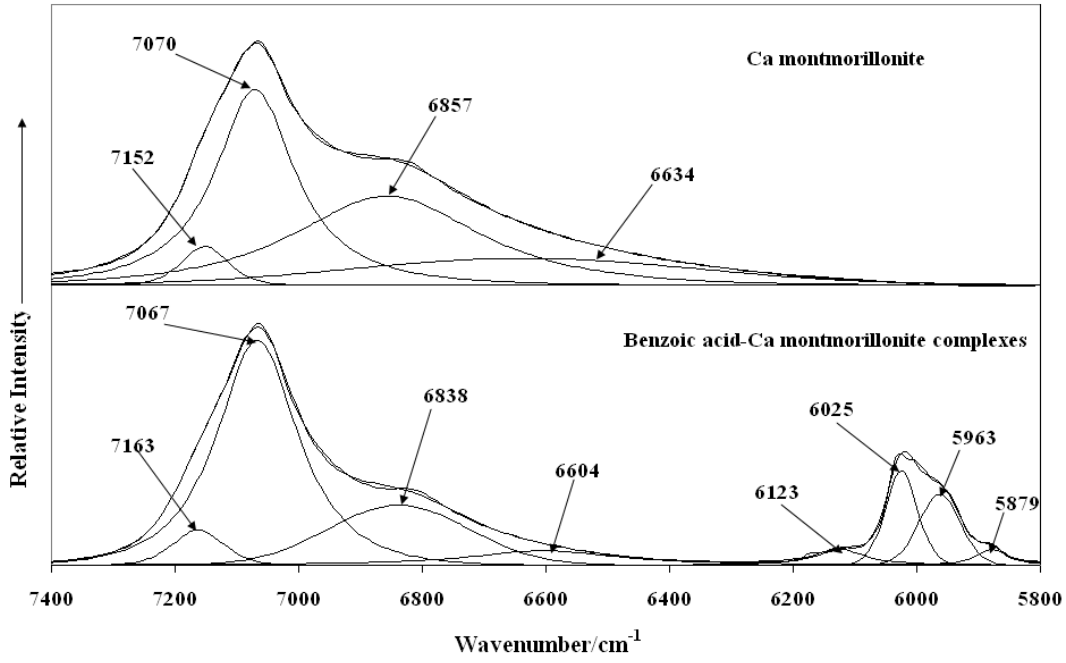

321

322

323 **Figure2b**

324

325

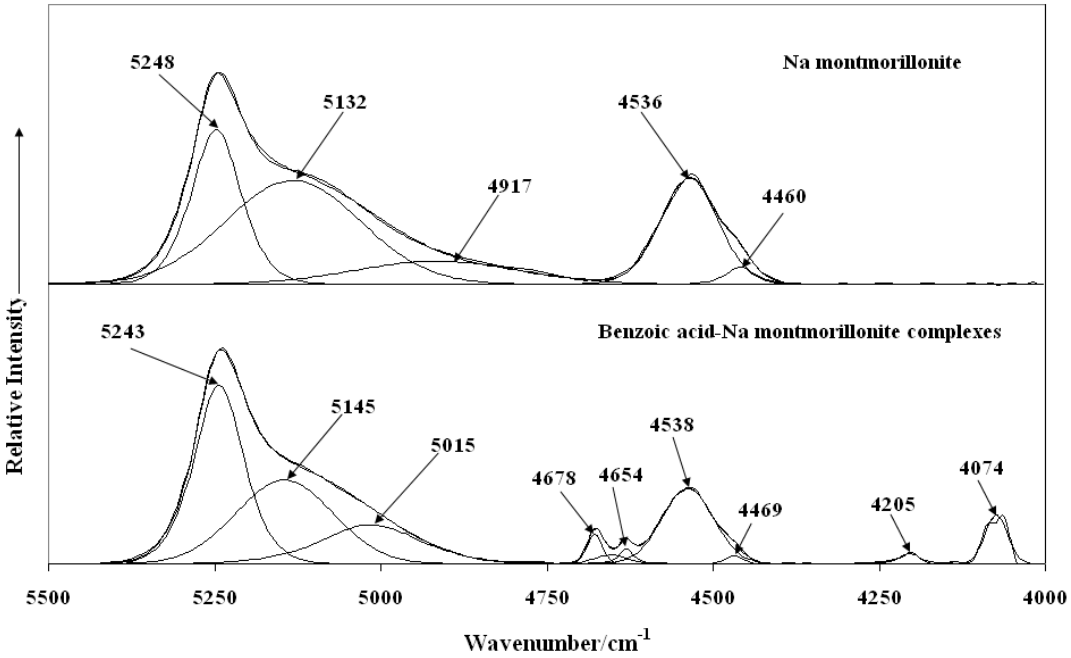

Figure 3a

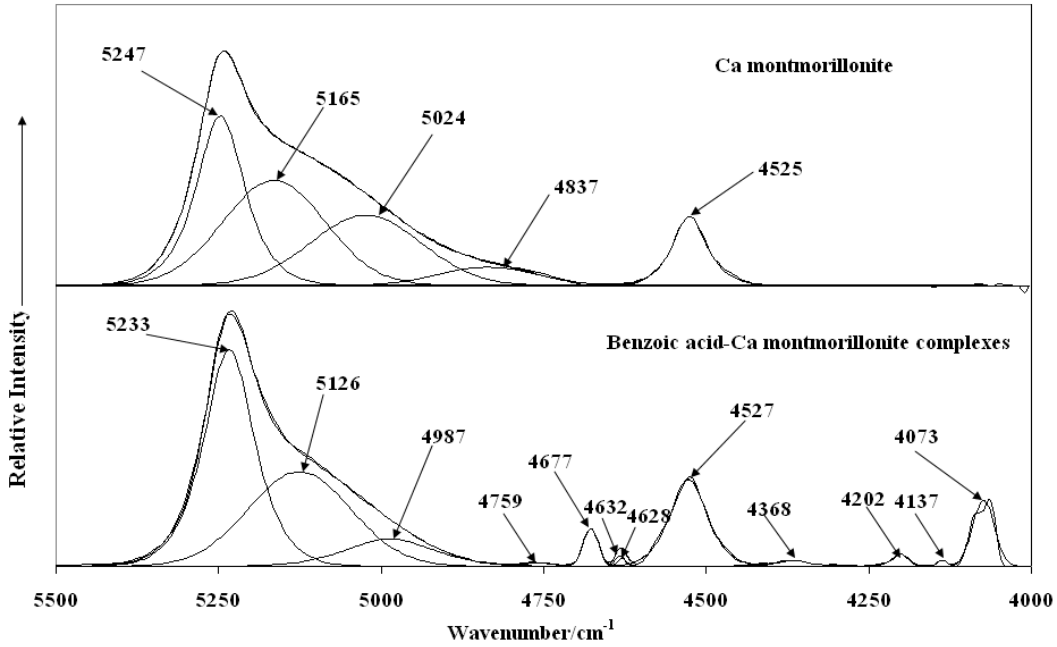

Figure 3b

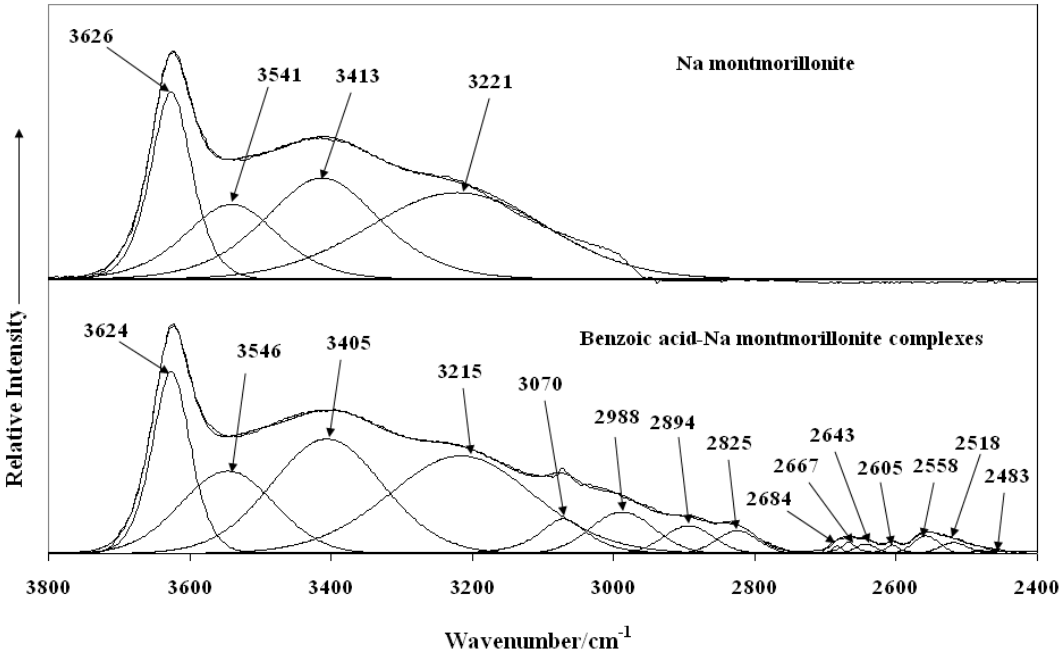

334

335

336 **Figure 4a**

337

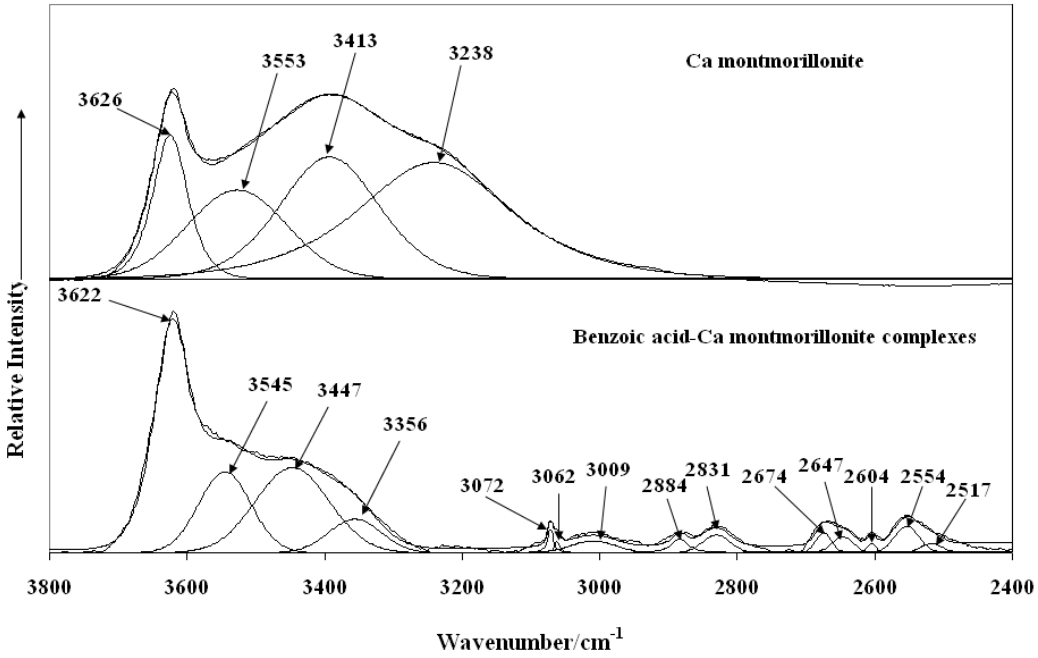

338

339 **Figure 4b**

340

341

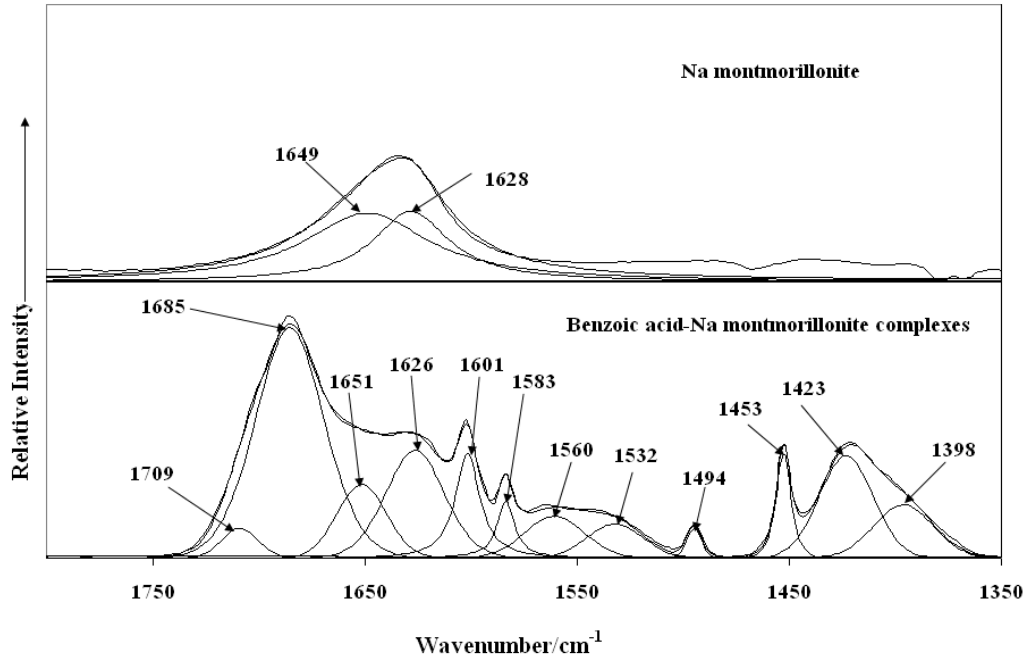

342

343 **Figure 5a**

344

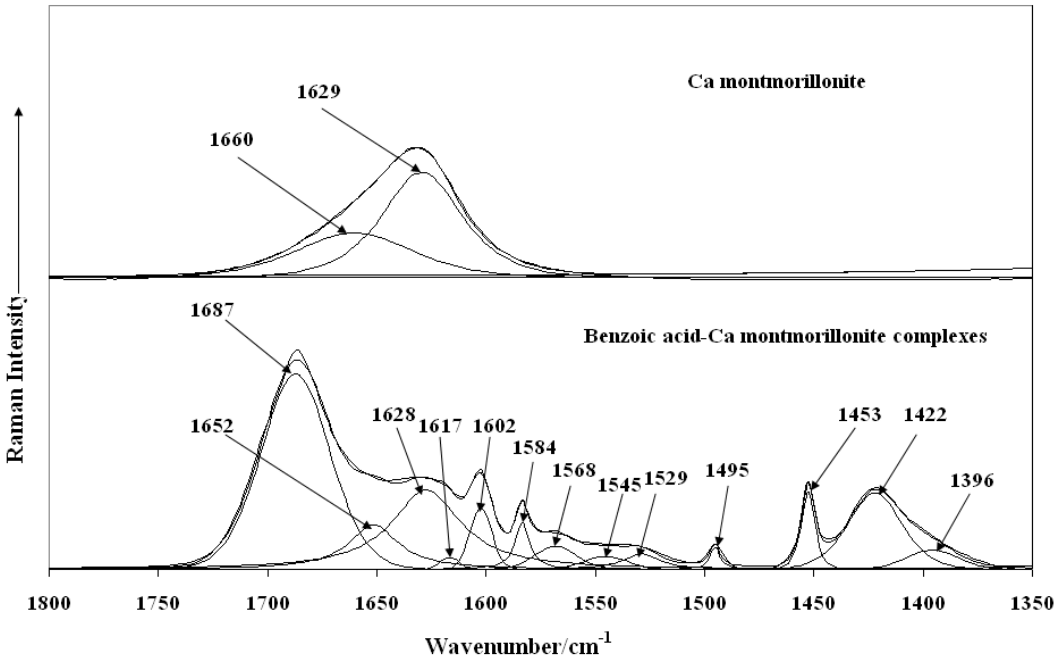

345

346

347 **Figure 5b**

348

349